AIAA JOURNAL
Vol. 41, No. 6, June 2003

Bursting Frequency Predictions for Compressible Turbulent Boundary Layers

William W. Liou* and Yichuan Fang†
Western Michigan University, Kalamazoo, Michigan 49008

A computational method for the prediction of the bursting frequency associated with the coherent streamwise structures in high-speed compressible turbulent boundary layers is presented. The structures are described as wavelike disturbances of the turbulent mean flow. A direct resonance theory is used to determine the frequency of bursting. The resulting hydrodynamic linear stability equations are discretized by using a Chebyshev collocation method. A global numerical method capable of resolving the entire eigenvalue spectrum is used. Realistic turbulent mean velocity and temperature profiles obtained by using a Reynolds-averaged Navier–Stokes equations solver and a two-equation turbulence model are applied. For all of the compressible turbulent boundary layers calculated, the results show at least one frequency that satisfies the resonance condition. A second frequency can be identified for cases with high Reynolds numbers.

Nomenclature

C	=	coefficient matrix
c	=	complex wave speed, ω/α
c_i	=	imaginary part of c
c_r	=	real part of c
D	=	lambda matrix
F	=	long-time average of f
f	=	instantaneous quantity
f'	=	short-time average of f
$\tilde{f}$	=	background fluctuation
i	=	$\sqrt{-1}$
M	=	Mach number
N	=	number of grid point
Re	=	Reynolds number, $\rho^*_\infty U^*_\infty \delta^*/\mu^*_\infty$
Re_δ	=	Reynolds number, $\rho^*_\infty U^*_\infty \delta/\mu^*_\infty$
s_p	=	grid stretching parameter
T	=	mean temperature
T_1	=	timescale for long-time average
T_2	=	timescale for short-time average
T'	=	wavelike temperature
U	=	mean streamwise velocity
u, v, w, p	=	velocity components and pressure
x, y, z	=	streamwise, wall-normal, and spanwise coordinates
Y	=	y^*/δ
$y_{\max}$	=	outer bound of the computational domain
α	=	complex streamwise wave number
β	=	spanwise wave number
β^+	=	$\beta^* \nu^*_\infty/u_\tau$
δ	=	boundary-layer thickness
δ^*	=	displacement thickness
η	=	wavelike vertical vorticity
μ, λ	=	fluid viscosity
ω	=	frequency, $\omega^* \delta^*/U^*_\infty$
ω^+	=	$\omega/(dU/dy)_{y=0}$

Subscript

∞	=	far field

Superscripts

$\hat{}$	=	eigenfunction
$*$	=	dimensional quantity

I. Introduction

LARGE-SCALE coherent structures have been observed in incompressible and compressible turbulent boundary layers. They exist in the near wall as well as the outer regions and are believed to be responsible for maintaining the turbulence in the boundary layer. Comprehensive reviews of their behaviors can be found in the literature.[1–4] In the near-wall region alternating streaks of low- and high-speed fluid (relative to the mean) have been observed,[5] supporting a view that counter-rotating streamwise vortices exist very near the wall. The quasi-deterministic occurrence of these large-scale organized structures and the production of turbulence associated with the violent eruption of the near-wall fluid are collectively referred to as the bursting process. The fluid dynamic processes described by the term bursting vary slightly since its first use.[6] It is, nevertheless, generally believed that the bursting process is of critical importance to the development of turbulent boundary layers.

Because of the necessary resolution of scales, experimental results focusing on the near-wall region are primarily limited to low Reynolds numbers and subsonic speeds. The spanwise spacing of the near-wall structures has been reported to be about 100 based on the near-wall viscous length scale by many experiments.[5,7] The frequency of bursting has also been of intense interests. Partly because of the subjective nature of the current experimental methods devised to detect the bursting process, there is less of a consensus regarding the frequency of the bursting process and its scaling.[8] As most of the turbulence production in the boundary layer occurs in the near-wall region,[9] the timescale of the bursting process is dynamically important to further a fundamental understanding of the development of turbulent boundary layers.

The frequency of bursting is of practical interests to high-speed aerospace applications. The sheath of plasma developed on the surface of a reentry vehicle can become turbulent and affect flight control. The dynamics of the boundary-layer structures can also be important in the acoustic noise generation and propagation from high-speed engines.

Computational models for the coherent near-wall structures in incompressible turbulent boundary layers have been proposed.[10–12] It

Presented as Paper 2002-0576 at the AIAA 40th Aerospace Sciences Meeting, Reno, NV, 14–17 January 2002; received 3 June 2002; revision received 13 January 2003; accepted for publication 21 January 2003.

*Associate Professor, Department of Mechanical and Aeronautical Engineering. Senior Member AIAA.

†Doctoral Associate, Department of Mechanical and Aeronautical Engineering. Student Member AIAA.

has been shown[13] that the statistically dominant streamwise fluctuation exhibits wave-like characteristics, suggesting that a hydrodynamic wave description for the streamwise structures can be applicable. Models based on hydrodynamic stability theory for the coherent structures in both the outer- and the near-wall regions of flat-plate boundary layers were reported.[11,12] Jang et al.[10] proposed a direct resonance theory to describe the bursting events. The structures are described as wavelike disturbances of the turbulent mean flow. They argued that, based on a weakly nonlinear analysis, resonance between the vertical velocity and the free mode of the vertical vorticity equations could occur. Using a temporal stability analysis and a shooting method, they have predicted a bursting frequency, nondimensionalized by the viscous scales, of 0.09 for incompressible turbulent boundary layers, which agrees well with experiment data.[13] They have also showed that the secondary mean flow induced by the resonant discrete mode contains streamwise vortical structures. The shape of the predicted structure and the spacing of the accompanying low-speed streaks are comparable to those observed in experiments. The direct resonance model has been applied to examine the more realistic spatially developing disturbances in incompressible turbulent boundary layers.[14] A numerical solver BURFIT has been developed. The calculated bursting frequency is 0.0962.

Note that a linear analysis has been used, with the calculated turbulent mean velocity profiles as the basic flow, to approximate the local characteristics of the coherent large-scale structures in incompressible turbulent free mixing layers.[15] A three-component decomposition of the flow quantities, the same as that used in the present study [Eq. (1)], was applied, and a predictive turbulence closure model was developed by describing the dynamics of the large-scale coherent structures with a weakly nonlinear theory. The results show that the calculated mean velocity, the Reynolds shear stress, and the dynamic evolution of the structures agree well with experiments. This and the other studies just cited indicate that the instability wave descriptions of the coherent structures are viable models for simple free and bounded shear layers.

In this paper a computational method for the prediction of the bursting frequency in compressible turbulent boundary layers is presented. The methodology is developed based on an extension of the incompressible direct resonance model[10] to high-speed boundary layers. The result will show that the present compressible formulation predicts the same bursting frequency as that obtained in Liou et al.[14] for incompressible turbulent boundary layers. Therefore, the present formulation is applicable to both incompressible and compressible turbulent boundary layers. It is not our intention here to build a turbulence closure model for the mean flow or the dynamic evolution of the streamwise coherent structures in compressible boundary layers.

It is stated in Morkovin's hypothesis[16] that "the essential dynamics of these shear flows will follow the incompressible pattern" for small fluctuating Mach numbers. In the absence of strong sources of mass and heat, the hypothesis has been found applicable to boundary layers of freestream Mach numbers less than 4 or 5 (Ref. 2). The hypothesized dynamic similarity between the incompressible and the compressible turbulent boundary layers is invoked in this exploratory application of the direct resonance theory to the compressible regime. The observed wavelike characteristics of the coherent near-wall structure in incompressible turbulent boundary layers are then assumed valid for compressible turbulent boundary layers. Fluid property variations accompanying that of temperature are considered. There might be other compressibility effects that play a role in the near-wall region of supersonic turbulent boundary layers where the flow gradients are large. There is, however, little substantive experimental evidence to support such conjectures.

In the following section the present compressible formulation of the direct resonance model and the numerical methods used are described. Results are presented for compressible boundary layers with various Reynolds numbers and freestream Mach numbers.

II. Formulation

Turbulence quantities f are decomposed into three components[10,15]:

$$f = F + f' + \breve{f} \tag{1}$$

A long-time average for f can be defined as

$$F = \frac{1}{T_1}\int_0^{T_1} f\,\mathrm{d}t \tag{2}$$

and the wavelike component f' can be obtained by using a short-time average

$$F + f' = \frac{1}{T_2}\int_0^{T_2} f\,\mathrm{d}t \tag{3}$$

where T_2 is much smaller than T_1 but much larger than the timescale of the background fluctuations $\breve{f}$. The equations for the wavelike components can be obtained by subtracting the long-time-averaged from the short-time-averaged Navier–Stokes equations. A normal mode solution is assumed for the spatially developing wavelike disturbances in a locally parallel mean flow, that is,

$$(u', v', w', p', T') = [\hat{u}(y), \hat{v}(y), \hat{w}(y), \hat{p}(y), \hat{T}(y)] \times \exp[i(\alpha x + \beta z - \omega t)] \tag{4}$$

If one substitutes Eq. (4) into the linearized equations for the wavelike component, the equations governing the mode shapes of the three velocity components, pressure, and temperature become

$$\frac{\gamma M^2}{T}\hat{p}(-i\omega) - \frac{1}{T^2}\hat{T}(-i\omega) + \frac{1}{T}\hat{u}(i\alpha) + U\left[\frac{\gamma M^2}{T}\hat{p}(i\alpha) - \frac{1}{T^2}\hat{T}(i\alpha)\right] + \frac{1}{T}\frac{\mathrm{d}\hat{v}}{\mathrm{d}y} - \frac{1}{T^2}\frac{\mathrm{d}T}{\mathrm{d}y}\hat{v} + \frac{1}{T}\hat{w}(i\beta) = 0 \tag{5a}$$

$$\frac{[\hat{u}(-i\omega) + U\hat{u}(i\alpha) + \hat{v}(\mathrm{d}U/\mathrm{d}y)]}{T} = -\hat{p}(i\alpha) + \frac{\mu}{Re}\left\{l_2(-\alpha^2)\hat{u} + l_1\left[\frac{\mathrm{d}\hat{v}}{\mathrm{d}y}(i\alpha) + \hat{w}(-\alpha\beta)\right] + \frac{\mathrm{d}^2\hat{u}}{\mathrm{d}y^2} + \hat{u}(-\beta^2) + \frac{1}{\mu}\frac{\mathrm{d}\mu}{\mathrm{d}T}\frac{\mathrm{d}T}{\mathrm{d}y}\left[\frac{\mathrm{d}\hat{u}}{\mathrm{d}y} + \hat{v}(i\alpha)\right] + \frac{1}{\mu}\frac{\mathrm{d}\mu}{\mathrm{d}T}\left[\frac{\mathrm{d}^2U}{\mathrm{d}y^2}\hat{T} + \frac{\mathrm{d}U}{\mathrm{d}y}\frac{\mathrm{d}\hat{T}}{\mathrm{d}y}\right] + \frac{1}{\mu}\frac{\mathrm{d}^2\mu}{\mathrm{d}T^2}\frac{\mathrm{d}T}{\mathrm{d}y}\frac{\mathrm{d}U}{\mathrm{d}y}\hat{T}\right\} \tag{5b}$$

$$\frac{[\hat{v}(-i\omega) + U\hat{v}(i\alpha)]}{T} = -\frac{\mathrm{d}\hat{p}}{\mathrm{d}y} + \frac{\mu}{Re}\left\{\hat{v}(-\alpha^2) + l_1\left[\frac{\mathrm{d}\hat{u}}{\mathrm{d}y}(i\alpha) + \frac{\mathrm{d}\hat{w}}{\mathrm{d}y}(i\beta)\right] + l_2\frac{\mathrm{d}^2\hat{v}}{\mathrm{d}y^2} + \hat{v}(-\beta^2) + \frac{1}{\mu}\frac{\mathrm{d}\mu}{\mathrm{d}T}\frac{\mathrm{d}U}{\mathrm{d}y}\hat{T}(i\alpha) + \frac{1}{\mu}\frac{\mathrm{d}\mu}{\mathrm{d}T}\frac{\mathrm{d}T}{\mathrm{d}y}\left[l_0\hat{u}(i\alpha) + \hat{w}(i\beta)\right] + l_2\frac{\mathrm{d}\hat{v}}{\mathrm{d}y}\right\} \tag{5c}$$

$$\frac{[\hat{w}(-i\omega) + U\hat{w}(i\alpha)]}{T} = -\hat{p}(i\beta) + \frac{\mu}{Re}\left\{\hat{w}(-\alpha^2) + l_1\left[\hat{u}(-\alpha\beta) + \frac{\mathrm{d}\hat{v}}{\mathrm{d}y}(i\beta)\right] + \frac{\mathrm{d}^2\hat{w}}{\mathrm{d}y^2} + l_2\hat{w}(-\beta^2) + \frac{1}{\mu}\frac{\mathrm{d}\mu}{\mathrm{d}T}\frac{\mathrm{d}T}{\mathrm{d}y}\left[\hat{v}(i\beta) + \frac{\mathrm{d}\hat{w}}{\mathrm{d}y}\right]\right\} \tag{5d}$$

$$\frac{[\hat{T}(-i\omega) + U\hat{T}(i\alpha) + \hat{v}(\mathrm{d}T/\mathrm{d}y)]}{T}$$

$$= (\gamma - 1)M^2[\hat{p}(-i\omega) + U\hat{p}(i\alpha)] + \frac{\mu}{RePr}\left\{\hat{T}(-\alpha^2 - \beta^2) + \frac{\mathrm{d}^2\hat{T}}{\mathrm{d}y^2} + \frac{2}{k}\frac{\mathrm{d}k}{\mathrm{d}T}\frac{\mathrm{d}T}{\mathrm{d}y}\frac{\mathrm{d}\hat{T}}{\mathrm{d}y} + \left[\frac{1}{k}\frac{\mathrm{d}k}{\mathrm{d}T}\frac{\mathrm{d}^2T}{\mathrm{d}y^2} + \frac{1}{k}\frac{\mathrm{d}^2k}{\mathrm{d}T^2}\left(\frac{\mathrm{d}T}{\mathrm{d}y}\right)^2\right]\hat{T}\right\}$$

$$+ (\gamma - 1)M^2\frac{\mu}{Re}\left\{2\frac{\mathrm{d}U}{\mathrm{d}y}\left[\frac{\mathrm{d}\hat{u}}{\mathrm{d}y} + \hat{v}(i\alpha)\right] + \frac{1}{\mu}\frac{\mathrm{d}\mu}{\mathrm{d}T}\left(\frac{\mathrm{d}U}{\mathrm{d}y}\right)^2\hat{T}\right\} \tag{5e}$$

Equation (5) has been nondimensionalized by using the freestream quantities F_∞ and the boundary-layer displacement thickness δ^*. $l_j(= j + \lambda/\mu)$ represent constants related to the fluid viscosity, μ and λ. The cross correlations between the turbulent fluctuations have been neglected because of their assumed disparate timescales. The Reynolds stresses associated with the random background fluctuation are also neglected in the formulation, as the transport processes are assumed predominantly large scale. Equation (5) governs the mode shapes of the wavelike disturbances f' about the mean flow F in terms of the complex streamwise wave number α, the spanwise wave number β, the frequency ω, the flow Mach number M, and the Reynolds number Re. With these assumptions the resulting equations become the linear hydrodynamic stability equations for compressible fluid flows.[17,18]

In this study the bursting frequency ω of the coherent structures in compressible turbulent boundary layers is sought using the direct resonance model. The condition for direct resonance can be written as

$$c^{CME}(\alpha, \beta, M, Re) = c^{VV}(\alpha, \beta, M, Re) \tag{6}$$

where c^{CME} and c^{VV} represent the wave speeds associated with the continuity, momentum, and energy equation (CME) and the free mode of the vertical vorticity (VV) eigenvalue problems, respectively. The homogeneous part of the equation for the vertical vorticity can be written as

$$\left[i(\alpha U - \omega) - \frac{T\mu}{Re}\left(\frac{\mathrm{d}^2}{\mathrm{d}y^2} + \frac{1}{\mu}\frac{\mathrm{d}\mu}{\mathrm{d}T}\frac{\mathrm{d}T}{\mathrm{d}y}\frac{\mathrm{d}}{\mathrm{d}y} - \alpha^2 - \beta^2\right)\right]\hat{\eta} = 0 \tag{7}$$

In this study the mean velocity and temperature profiles of the turbulent boundary layers have been obtained from the numerical solutions of a Navier–Stokes equation solver[19] and a k–ε turbulence model.[20] Efforts were taken to ensure convergence in not only the U and T profiles but also their derivatives that were used in the stability equations.

The boundary conditions on the isothermal wall are

$$\hat{u} = \hat{v} = \hat{T} = \hat{w} = 0 \tag{8}$$

A wall boundary condition for the pressure disturbance can be obtained by substituting Eq. (8) into Eq. (5c). The resulting equation can be written as

$$\frac{\partial\hat{p}}{\partial y} = \frac{\mu}{R}\left[l_1\left(i\alpha\frac{\partial\hat{u}}{\partial y} + i\beta\frac{\partial\hat{w}}{\partial y}\right)\right] + l_2\frac{\partial^2\hat{v}}{\partial y^2} + \frac{1}{\mu}\frac{\mathrm{d}\mu}{\mathrm{d}T}\frac{\mathrm{d}T}{\mathrm{d}y}l_2\frac{\partial\hat{v}}{\partial y} \tag{9}$$

The boundary conditions at the freestream are that all disturbances vanish at the far field.

III. Numerical Methods

Various numerical methods for solving the stability equations like Eqs. (5) and (7) have been used in the literature.[17,18,21–26] In the present study the equations have been discretized by applying the Chebyshev collocation method.[27] The Gauss–Lobatto collocation points are used in this study:

$$\bar{y}_i = \cos(\pi i/N) \qquad (i = 0, 1, \ldots, N) \tag{10}$$

An algebraic mapping has been applied to map the Chebyshev domain $\bar{y} \in [-1, 1]$ to the semi-infinite physical domain y:

$$y = \frac{y_{\max}s_p(1 + \bar{y})}{2s_p + y_{\max}(1 - \bar{y})} \tag{11}$$

where s_p denotes a stretching parameter, which determines the grid point clustering near the wall and $y_{\max}$ the outer bound in the far field. The resulting homogeneous system of equations forms an eigenvalue problem that is nonlinear in the parameter α. For Eq. (5) it can be written as

$$D_2(\alpha)\tilde{f} = 0 \tag{12}$$

where $\tilde{f}$ denotes a vector containing the solution variables $(\hat{u}, \hat{v}, \hat{w}, \hat{p}, \hat{T})$ at the collocation points. The matrix D_2 represents a lambda matrix of degree two and can be expressed as a scalar polynomial with matrix coefficients:

$$D_2(\alpha) = C_0\alpha^2 + C_1\alpha + C_2 \tag{13}$$

With the inclusion of the boundary conditions, the matrices C become square matrices of order $5 \times (N + 1)$. A linear companion matrix method[28] is used to linearize the lambda matrix. The eigenvalue problem has been solved by using the subroutine ZGEEV of LAPACK. For Eq. (7) the system of equations can be written in the same form as Eq. (12). The eigenvalue problem can be solved by using the procedure just outlined.

The resonance in the stability problem occurs when there is a set of parameters (α, β, ω) for which the solution of Eqs. (5) and (7) exist for given distributions of the mean velocity and temperature, the Mach number, and the Reynolds number. To locate the resonance mode, the following form of Eq. (6) is solved:

$$c_r^{CME}(\alpha, \beta, M, Re) - c_r^{VV}(\alpha, \beta, M, Re) = 0 \tag{14a}$$

$$c_i^{CME}(\alpha, \beta, M, Re) - c_i^{VV}(\alpha, \beta, M, Re) = 0 \tag{14b}$$

In the following section results of the validation of the numerical tools are first described. The predictions of bursting frequency in compressible turbulent boundary layers of different Mach numbers and Reynolds numbers are presented.

IV. Results

A. Validation

The linear stability problems of Eqs. (5) and (7) have been solved using the Chebyshev collocation method. To validate the numerical solver developed for this study, the linear stability results for incompressible and compressible boundary layers have been computed and compared with earlier results. Comparisons are shown in Figs. 1 and 2 and Tables 1 and 2.

First, an analytical velocity profile

$$U = 2Y^2 - 2Y^3 + Y^4 \tag{15}$$

has been assumed. The use of Eq. (15) allows a direct validation of the numerical solver developed in the current study of compressible

Table 1 Comparison of the calculated eigenvalues for the Blasius boundary layer with $Re = 10^3$, $\omega = 0.07$, and $\beta = 0.12$ [$\alpha = (0.19861, -0.00420)$ (Ref. 28)]

N	α
21	(0.199086, −0.00242427)
41	(0.198624, −0.00420748)
81	(0.198611, −0.00420091)
201	(0.198610, −0.00420033)
301	(0.198610, −0.00420001)

Table 2 Comparison of the calculated eigenvalues for the supersonic boundary layer of $M = 4.5$ (Ref. 21) $Re = 1.5 \times 10^3$, $\omega = 0.23$, and $\beta = 0$

Calculation	Eigenvalue
Present	(0.253406, −0.00249213)
Malik[21]	
MDSP[a]	(0.2534048, −0.0024921)
4CD[b]	(0.2534081, −0.0024932)
Chang[24]	
4CTD[c]	(0.253469, −0.00249491)

[a]MDSP = multidomain spectral collocation.
[b]4CD = fourth-order compact difference.
[c]4CTD = fourth-order central difference.

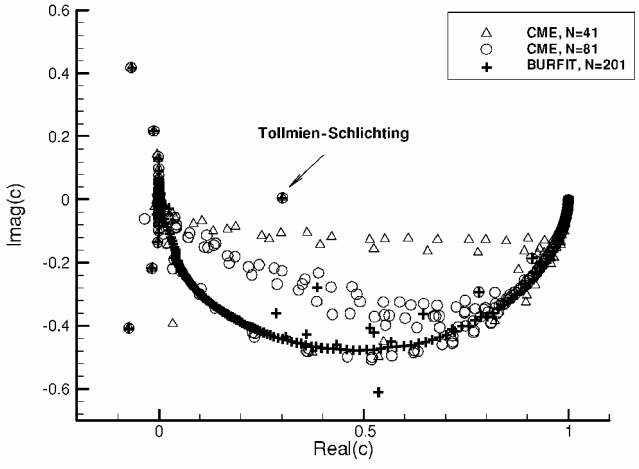

Fig. 1 Complex wave speed of Eq. (2): polynomial velocity profile.

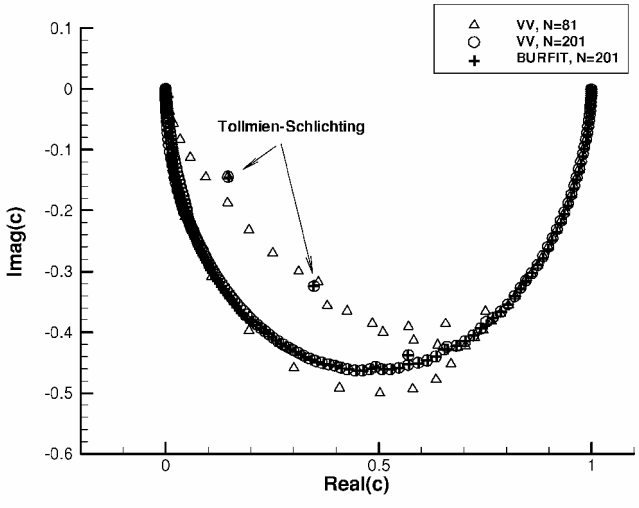

Fig. 2 Complex wave speed of Eq. (4): polynomial velocity profile.

boundary layers with that used for the incompressible cases.[14] The temperature distribution can be related to the velocity profile through the energy equation. The results can be written as

$$T = T_r\{r + (1 - r)U - (1 - 1/T_r)U^2\} \tag{16}$$

where T_r denotes the wall recover temperature and r the recovery factor ($= T_w/T_r$). For the present validation the freestream Mach number was set at 0.001.

Figure 1 shows the calculated wave-speed spectrum of Eq. (5) for a plane mode of $Re_\delta = 8 \times 10^3$ and $\omega = 0.2354$. The complex wave-speed spectra obtained by using the Chebyshev collocation method are given for various grid numbers. The result obtained by the incompressible BURFIT code has also been included for comparison. The Chebyshev collocation method shows a very good

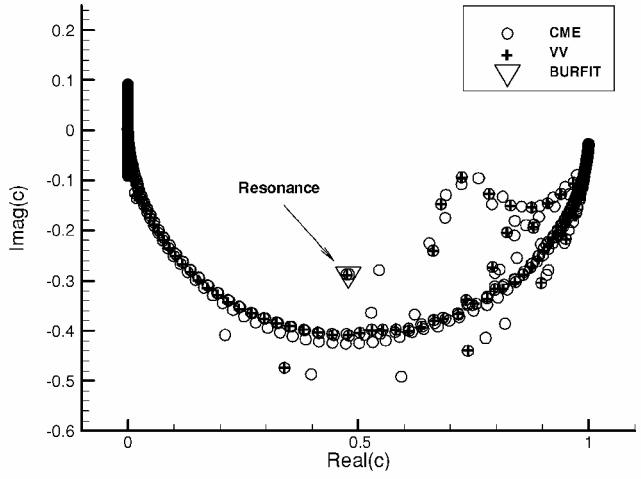

Fig. 3 Complex wave speed at resonance in an incompressible turbulent boundary layer.

prediction of the discrete spectrum with only 41 grid points. The continuous part of the spectrum is also seen to approach that from the incompressible code as the number of grid points increases. As can be seen in Fig. 2, for the free mode of the vertical vorticity equation the discrete spectrum is also resolved quite well for $N = 81$, and the continuous part of the spectrum overlaps that of the incompressible result for $N = 201$.

Table 1 shows a comparison of the calculated eigenvalues for the Blasius boundary layer with $Re = 10^3$, $\omega = 0.07$, and $\beta = 0.12$. The calculated discrete modes obtained by using various numbers of grid points are compared with previously published data.[28] There is a good agreement between the current calculations and the data, particularly for cases with a high number of grid points N. Table 2 shows a comparison of the calculated eigenvalues for a $M = 4.5$ supersonic boundary layer.[21] The present results obtained with $N = 121$ agree well those obtained by using the different numerical methods.[21,24]

B. Bursting Frequency Predictions

For an incompressible turbulent boundary layer with Re of 10^3, the bursting frequency ω^+ has been found to be 0.0962 (Ref. 14). Figure 3 shows the calculated eigenvalue spectrum at this resonance condition using the current solver. For comparison with the incompressible result, the temperature profile has been set uniform. An overlap of a discrete mode for the CME and the VV equations can be clearly identified, and the overlapped mode is in a good agreement with the resonance mode obtained by using the incompressible solver BURFIT.

To identify a resonance mode for compressible boundary layers, Eqs. (5) and (7) are first solved. Resonance occurs when the solution to the resonance condition, Eq. (14), is found. In the present study Eqs. (14a) and (14b) have been solved as a system of two equations nonlinear in the two variables α and β. The solution of the nonlinear system of equations has been obtained by using a LAPACK routine HYBRD, which finds the zero of a system of nonlinear functions by a modification of the Powell's hybrid algorithm,[29] a variation of Newton's method.

The compressible turbulent boundary layers studied here have been extensively examined and documented[30–32] and are appropriate to use in the present study. The surveyed station has a Reynolds number, based on the displacement thickness of 0.0063 m, of 4.21247×10^5. The associated eigenvalue spectra of Eqs. (5) and (7) are shown in Fig. 4, where the values of ω and β used have been determined by a viscous scaling of the ω^+ and β^+ of the incompressible resonance mode. Figure 4 shows that the eigenvalue spectra of Eqs. (5) and (7) consist of multiple discrete, damped modes, and none of the discrete modes satisfies Eq. (14), which, according to the direct resonance model, identifies the bursting frequency. The result indicates that the near-wall viscous scaling is not appropriate for correlating the bursting frequency in incompressible turbulent

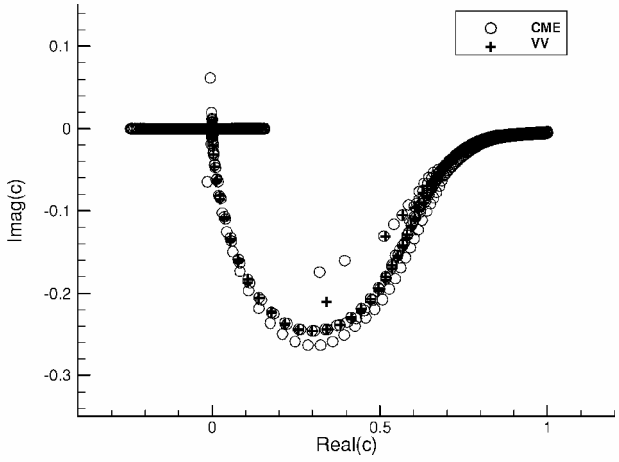

Fig. 4 Wave-speed spectra of the compressible turbulent boundary layer: $M = 2.85$, $Re = 4.21247 \times 10^5$, and $\omega = 8.2706$.

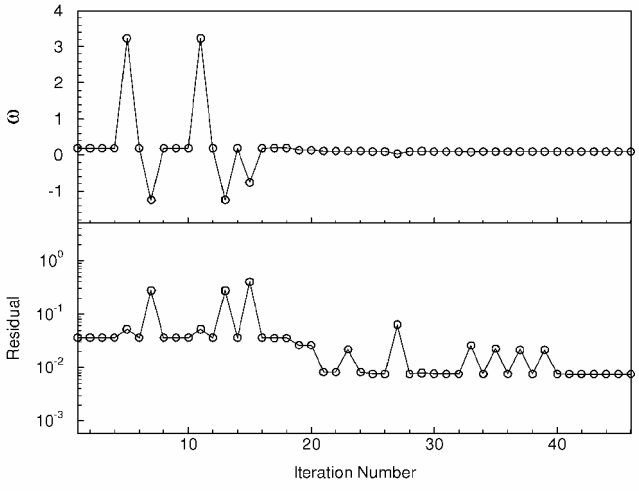

Fig. 5 History of convergence: $M = 4$ and $Re = 4.21247 \times 10^5$.

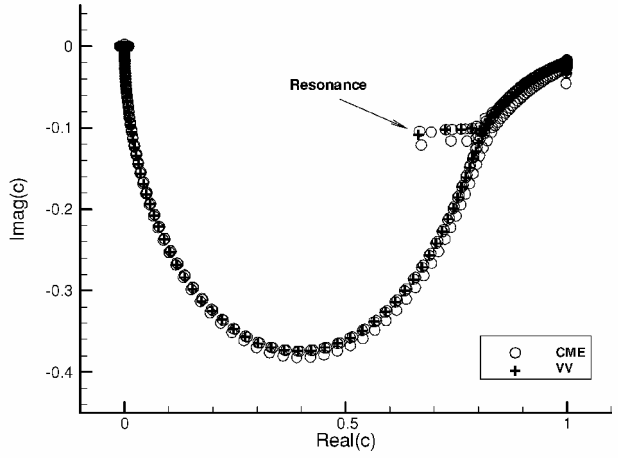

Fig. 6 Wave-speed spectra at bursting frequency 1 in the compressible turbulent boundary layer: $M = 2.85$, $Re = 4.21247 \times 10^5$, $\omega = 0.104$, and $N = 170$.

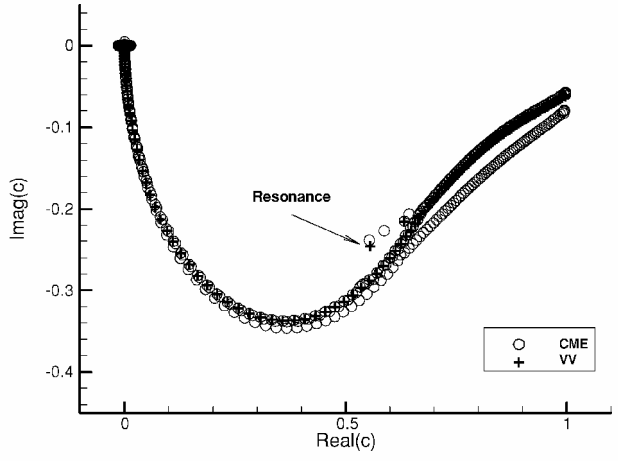

Fig. 7 Wave-speed spectra at bursting frequency 2 in the compressible turbulent boundary layer: $M = 2.85$, $Re = 4.21247 \times 10^5$, and $\omega = 0.659$.

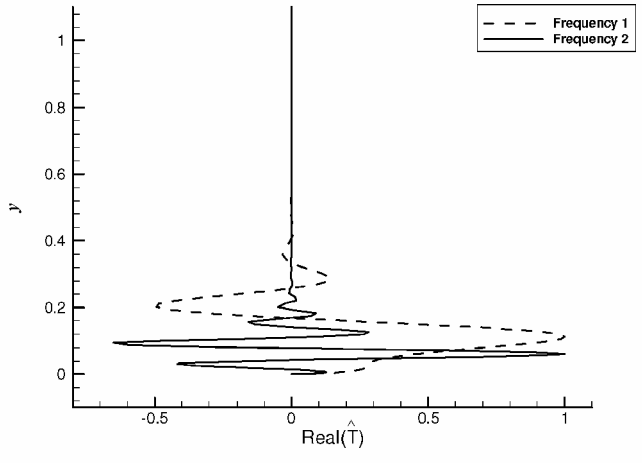

Fig. 8 Temperature mode shapes: $M = 2.85$ and $Re = 4.21247 \times 10^5$.

boundary layers with that in the compressible turbulent boundary layer studied here. Because the asymptotic forms of both equations at the far field admit oscillatory, decaying solutions, there is an overlap of the continuous part of the spectra[25,33] for all frequencies. This overlap of the continuous spectra, as is shown in Fig. 4, is not considered in solving Eq. (14) in the present study.

To locate the bursting frequency in the supersonic boundary layers, Eqs. (5), (7), and (14) were solved as just described. In this study possibilities for resonance to occur to the least damped mode with the lowest wave speed were examined. It can be argued that this is the mode that is most likely to be involved in a resonance. The iteration or the search for the resonance mode has been performed by solving Eqs. (5), (7), and (14) at every iteration step. The initial estimates of ω and β were obtained by trial and error. Because of the nonlinear nature of these equations, the iterative solution process is time consuming, especially when the initial values of ω and β have not been set appropriately. In this study the iteration is considered complete when the L_2 norm of the residual of Eq. (14), or $\sqrt{[(c_r^{CME} - c_r^{VV})^2 + (c_i^{CME} - c_i^{VV})^2]}$, has dropped below 10^{-2}. Figure 5 shows a typical history of convergence, which takes nearly 50 iterations to complete. The iteration begins with $\omega = 0.178$ and $\beta = 49.213$. The converged values are $\omega = 0.104$ and $\beta = 26.902$.

For the supersonic boundary layer of Mach number 2.85 and the Reynolds number of 4.21247×10^5, two bursting frequencies have been identified. The values of ω are 0.104 (frequency 1) and 0.659 (frequency 2), respectively. The corresponding dimensional frequencies are 1.515 kHz for frequency 1 and 9.605 kHz for frequency 2. The values of β are 26.904 and 126.324, respectively. Their eigenvalue spectra are shown in Figs. 6 and 7. The wave speed associated with frequency 2 is located closer to the continuous part of its spectrum than that of frequency 1. Figure 8 shows the distributions of the real parts of the mode shapes for the temperature associated with frequencies 1 and 2. The temperature eigenfunctions have been normalized by their respective maximum values. The temperature mode shape for frequency 2 shows a higher level of oscillation compared with that of frequency 1. Modes of frequency 2 then can be associated with wavelike fluctuations of smaller length and timescales. Attempts have also been made to find solutions of Eq. (14) based on the other discrete modes. These searches failed

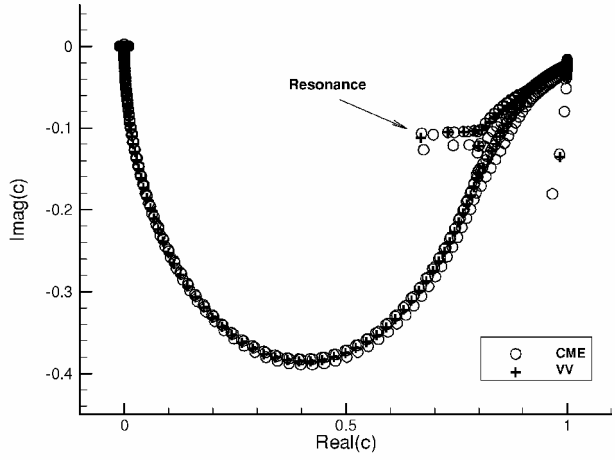

Fig. 9 Wave-speed spectra at bursting frequency 1 in the compressible turbulent boundary layer: $M = 2.85$, $Re = 4.21247 \times 10^5$, $\omega = 0.104$, and $N = 200$.

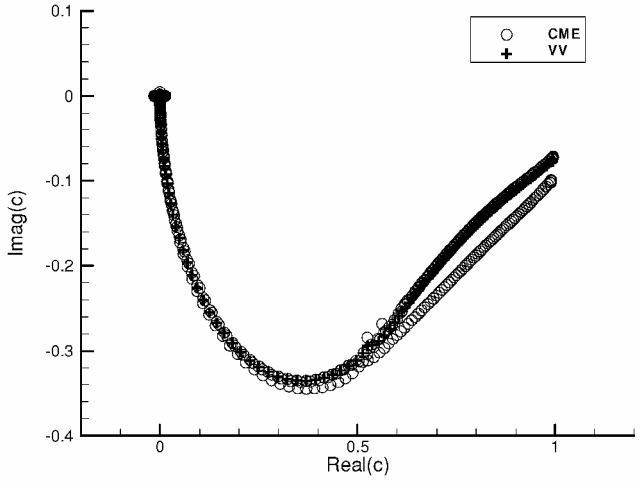

Fig. 11 Complex wave-speed spectra for a compressible turbulent boundary layer: $M = 2.85$ and $Re = 3.74466 \times 10^5$.

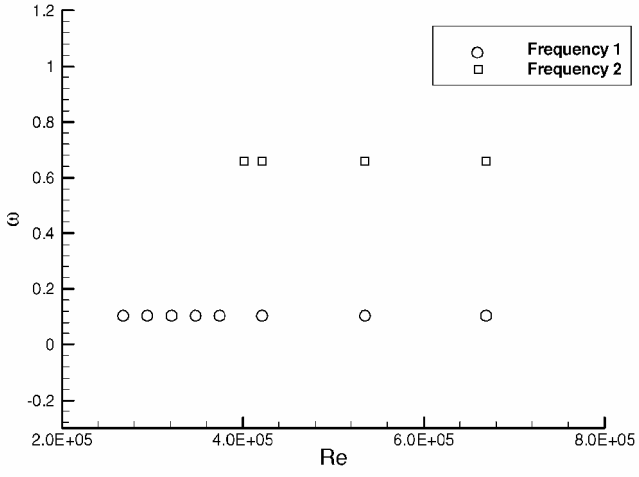

Fig. 10 Bursting frequencies in the compressible turbulent boundary layers: $M = 2.85$.

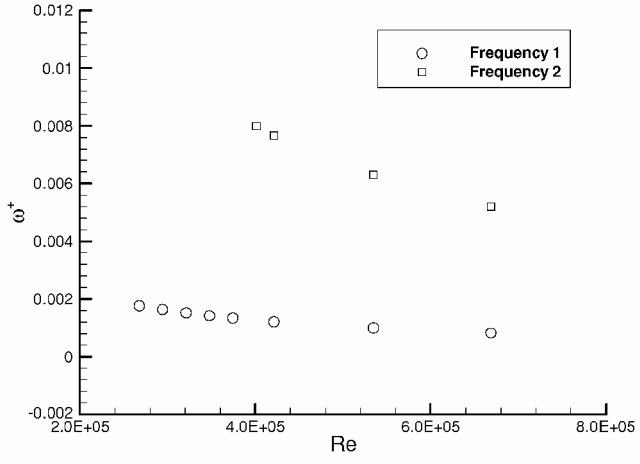

Fig. 12 Bursting frequency in the compressible turbulent boundary layers.

to identify any additional bursting frequencies. Note that the number of grid points used is 170, and the computed eigenvalues do not change in any significant way with reasonable changes in other parameters, such as the value of s_p and the size of the computational domain. For example, Fig. 9 shows the eigenvalue spectra for frequency 1 with 200 grid points. The spectra compare well with those in Fig. 6, which have been obtained by using 170 grid points. The results presented in Figs. 6–8 and in the following have been obtained with $s_p = 0.5$ and Fig. 9 with $s_p = 1.0$. Calculations with s_p varying from 0.1 to 2.0 yield essentially the same solutions.

The effect of the Reynolds number on the bursting frequency predictions is shown in Fig. 10. For all of the Reynolds numbers calculated, ranging between 2.67475×10^5 and 6.68689×10^5, the low frequency of 0.104 satisfies the resonance condition. It appears to be not sensitive at all to the changes in the Reynolds number. The high bursting frequency (frequency 2) identified for $Re = 4.21247 \times 10^5$ has also been found to satisfy the resonance condition and its value to be insensitive to the variation of the Reynolds number. This is true, however, only for large Reynolds numbers, in this case, higher than 4.01216×10^5. For boundary layers of lower Reynolds numbers, the iteration procedure just described has not identified a converged solution near frequency 2 ($\omega = 0.659$). For example, the eigenvalue spectra for $Re = 3.74466 \times 10^5$ at frequency 2 are shown in Fig. 11. Neither the spectrum of Eq. (5) nor that of Eq. (7) appears to have any discrete mode that can be identified with ease. Figure 12 shows the variation of ω^+ with the Reynolds numbers. A gradual decrease with the Reynolds number can be observed for both frequencies. Overall, the values of ω^+ for the compressible cases tested are one order of magnitude smaller than that in incompressible turbulent boundary layers,[14] mainly because of the high skin-friction velocities.

The freestream Mach number has been increased to 4.0 while keeping the Reynolds number at 4.21247×10^5 by reducing the displacement thickness of the boundary layer. The results show that frequency 1 ($\omega = 0.104$) remains a resonance frequency for this particular boundary layer. The history of convergence for this calculation has been shown in Fig. 5. On the other hand, the iteration procedure did not converge to a solution that satisfied Eq. (14) near frequency 2. Recall that, for the same Reynolds number, both frequencies have been identified as the bursting frequencies 1 and 2 in the boundary layer with a 2.85 freestream Mach number. It then appears that one of the two bursting frequencies does not scale with the outer timescale δ^*/U_∞^*.

V. Summary

The paper describes a computational method for the prediction of the bursting frequency in high-speed, compressible turbulent boundary layers. It is developed based on the direct resonance theory. The linear stability solver developed has been validated for the linear stability of incompressible and compressible boundary layers. The computational method has been applied to compressible boundary layers of various Reynolds numbers and Mach numbers. The results suggest possible multiple frequencies of bursting in the compressible boundary layers calculated.

Although there is evidence indicating that the computational method developed in this study for compressible boundary layers produces in a satisfactory manner information obtained in a

high-speed flight test, there is a need for more complete and accurate compressible experimental data to further assess the approach. Until such compressible near-wall flow structure data become available, the present computational method represents a unique way to meet the current demand for an engineering prediction capability for the bursting frequency in incompressible and compressible turbulent boundary layers. In addition, the results of this study can also serve as a guide for future experimental studies of high-speed turbulent boundary layers.

Acknowledgments

The work is supported by Sandia National Laboratories under Contract 14335. Roy S. Baty and Donald L. Potter are the Technical Monitors.

References

[1]Robinson, S., "Coherent Motions in the Turbulent Boundary Layer," *Annual Review of Fluid Mechanics*, Vol. 23, 1991, pp. 601–639.

[2]Spina, E. F., Smits, A. J., and Robinson, S. K., "The Physics of Supersonic Turbulent Boundary Layers," *Annual Review of Fluid Mechanics*, Vol. 26, 1994, pp. 287–319.

[3]Panton, R. L. (ed.), *Self-Sustaining Mechanisms of Wall Turbulence*, Computational Mechanics Publications, 1997.

[4]Smith, C. R., Walker, J. D. A., Haidari, A. H., and Sobrun, U., "On the Dynamics of Near-Wall Turbulence," *Philosophical Transactions of the Royal Society of London A*, Vol. 336, 1991, pp. 131–175.

[5]Kline, S. J., Reynolds, W. C., Schraub, F. A., and Runstadler, P. W., "The Structure of Turbulent Boundary Layers," *Journal of Fluid Mechanics*, Vol. 30, 1967, pp. 741–773.

[6]Runstadler, P. W., Kline, S. J., and Reynolds, W. C., "An Experimental Investigation of Flow Structure of the Turbulent Boundary Layer," Mechanical Engineering Dept., Stanford Univ., Rept. MD-8, Stanford, CA, 1963.

[7]Kim, H. T., Kline, S. J., and Reynolds, W. C., "The Production of Turbulence near a Smooth Wall in a Turbulent Boundary Layer," *Journal of Fluid Mechanics*, Vol. 50, 1971, pp. 133–160.

[8]McComb, W. D., *The Physics of Fluid Turbulence*, Clarendon, Oxford, 2000.

[9]Klebanoff, P. S., "Characteristics of Turbulence in a Boundary Layer with Zero Pressure Gradient," NACA Rept. 1247, 1955.

[10]Jang, P. S., Benny, D. J., and Gran, R. L., "On the Origin of Streamwise Vortices in a Turbulent Boundary Layer," *Journal of Fluid Mechanics*, Vol. 169, 1986, pp. 109–123.

[11]Zhang, Z. A., and Lilley, G. M., "A Theoretical Model of the Coherent Structure of the Turbulent Boundary Layer in Zero Pressure Gradient," *Turbulent Shear Flows* 3, edited by L. J. S. Bradbury, F. Durst, B. E. Launder, F. W. Schmidt, and J. H. Whitelaw, Springer-Verlag, New York, 1981, pp. 11.24–11.29.

[12]Zhou, H., and Luo, J.-S., "Theoretical Models for the Coherent Structures in a Turbulent Boundary Layer," *Near-Wall Turbulent Flows*, edited by R. M. C. So, C. G. Speziale, and B. E. Launder, Elsevier, 1993, pp. 537–546.

[13]Morrison, W. R. B., and Kronauer, R. E., "Structural Similarity for Fully Developed Turbulence in Smooth Tubes," *Journal of Fluid Mechanics*, Vol. 39, 1969, pp. 117–141.

[14]Liou, W. W., Fang, Y., and Baty, R. S., "Global Numerical Prediction of Bursting Frequency in Turbulent Boundary Layer," *International Journal of Numerical Method for Heat and Fluid Flow*, Vol. 10, 2000, pp. 862–876.

[15]Liou, W. W., and Morris, P. J., "Weakly Nonlinear Models for Turbulent Mixing in a Plane Mixing Layer," *Physics of Fluids*, Vol. 4, 1992, pp. 2798–2808.

[16]Morkovin, M. V., "Effects of Compressibility on Turbulent Flows," *Mechanique de la Turbulence*, edited by A. Favre, Centre National de la Recherche Scientifique, Paris, 1962, pp. 367–380.

[17]Lees, L., and Lin, C. C., "Investigation of the Stability of the Laminar Boundary Layer in a Compressible Fluid," NACA TN 1115, 1946.

[18]Mack, L. M., "Boundary Layer Linear Stability Theory," AGARD, Rept. 709, 1984, pp. 3-1–3-8.

[19]Liou, W. W., Huang, G., and Shih, T.-H., "Turbulence Model Assessment of Shock Wave/Turbulent Boundary-Layer Interaction in Transonic and Supersonic Flows," *Computers and Fluids*, Vol. 29, 2000, pp. 275–299.

[20]Chien, K. Y., "Predictions of Channel and Boundary Layer Flows with a Low Reynolds Number Turbulence Model," *AIAA Journal*, Vol. 20, 1982, pp. 33–38.

[21]Malik, M. R., "Numerical Methods for Hypersonic Boundary Layer Stability," *Journal of Computational Physics*, Vol. 86, 1990, pp. 376–413.

[22]Joslin, R. D., Morris, P. J., and Carpenter, P. W., "The Role of Three-Dimensional Instabilities in Compliant-Wall Boundary Layer Transition," *AIAA Journal*, Vol. 29, 1991, pp. 1603–1610.

[23]Chang, C.-L., and Malik, M. R., "Oblique-Mode Breakdown and Secondary Instability in Supersonic Boundary Layers," *Journal of Fluid Mechanics*, Vol. 273, 1994, pp. 323–360.

[24]Chang, C.-L., "The Langley Stability and Transition Analysis Codes (LASTRAC)—LST, Linear & Nonlinear PSE for 2D, Asixymmetric and Iinfinite Swept Wing Boundary Layers," AIAA Paper 2002-0974, Jan. 2002.

[25]Liou, W. W., and Morris, P. J., "The Eigenvalue Spectrum of the Rayleigh Equation for a Plane Shear Layer," *International Journal of Numerical Methods in Fluids*, Vol. 15, 1992, pp. 1407–1415.

[26]Bridges, T. J., and Morris, P. J., "Differential Eigenvalue Problems in Which the Parameter Appear Nonlinearly," *Journal of Computational Physics*, Vol. 55, 1984, pp. 437–460.

[27]Canuto, C., Hussaini, M. Y., Quarteroni, A., and Zang, T. A. (eds.), *Spectral Method in Fluid Dynamics*, Springer-Verlag, New York, 1987.

[28]Bridges, T. J., and Morris, P. J., "Boundary Layer Stability Calculations," *Physics of Fluids*, Vol. 30, 1987, pp. 3351–3358.

[29]Powell, M. J. D., "A Hybrid Method for Nonlinear Algebraic Equations," *Numerical Method for Nonlinear Algebraic Equations*, edited by. P. Rabinowitz, Gordon and Breach, New York, 1970.

[30]Spina, E. F., and Smits, A. J., "Organized Structures in a Compressible, Turbulent Boundary Layer," *Journal of Fluid Mechanics*, Vol. 182, 1987, pp. 85–100.

[31]Settles, G. S., and Dodson, L. J., "Hypersonic Shock/Boundary Layer Interaction Database," NASA CR 177577, 1991.

[32]Fernholz, H. H., Dussauge, J. P., Finley, P. J., and Smits, A. J., "A Survey of Measurements and Measuring Techniques in Rapidly Distorted Compressible Turbulent Boundary Layers," AGARDograph 315, 1989.

[33]Grosch, C. E., and Salwen, H., "The Continuous Spectrum of the Orr-Sommerfeld Equation. Part I. The Spectrum and the Eigenfunctions," *Journal of Fluid Mechanics*, Vol. 87, 1978, pp. 33–54.

W. J. Devenport
Associate Editor